Intrastrand Electron and Energy Transfer between Polypyridyl Complexes on a Soluble Polymer

Wayne E. Jones, Jr., Steven M. Baxter, Geoffrey F. Strouse, and Thomas J. Meyer*

Contribution from the Department of Chemistry, Venable and Kenan Laboratories, University of North Carolina, Chapel Hill, North Carolina 27599-3290

Received March 5, 1993

Abstract: Intrastrand electron and energy transfer between pendant sites in a derivatized 1:1 copolymer of styrene and *p*-(chloromethyl)styrene have been studied by laser flash photolysis. The polymer [*p*-PS-$Ru^{II}_{22}Os^{II}_{5}$]$(PF_6)_{54}$, in which 22 of the ~27 repeat units of an average strand were Ru^{II} and 5Os^{II}, was prepared by nucleophilic displacement of chloride by $[M(bpy)_2(bpyCH_2OH)]^{2+}$ (M is Ru or Os; bpy is 2,2′-bipyridine; $bpyCH_2OH$ is 4-Me-4′-CH_2OH-2,2′-bipyridine) under basic conditions. Following Ru^{II} → bpy laser flash excitation there was evidence for a rapid (τ < 5 ns) Ru^{II*} → Os^{II} energy transfer component with the remaining Ru^{II*} emission relatively unperturbed compared to [*p*-PS-Ru^{II}_{27}]$(PF_6)_{54}$. On the basis of these observations it was inferred that Ru^{II*} → Os^{II} energy transfer (which is spontaneous by 0.36 eV) does occur with $k(295 \pm 2K, CH_3CN) > 2 \times 10^8$ s^{-1}, *but only to Os^{II} sites that are adjacent to Ru^{II*}*. Energy transfer self-exchange from Ru^{II*} to Ru^{II} ($\Delta G° = 0.0$ eV) is slow with $k < 1 \times 10^6$ s^{-1}. In the presence of 35 mM of the irreversible, oxidative quencher [*p*-$CH_3OC_6H_4N_2$](BF_4) in CH_3CN ~95% of the emission from [*p*-PS-$Ru^{II}_{22}Os^{II}_{5}$]$(PF_6)_{54}$ is quenched. Transient absorption measurements under these conditions show an instantaneous loss of Os^{II} → bpy, Ru^{II} → bpy absorption (bleaching) in the visible, consistent with excitation and oxidative quenching during the laser pulse. Careful measurements at $\lambda > 500$ nm reveal a slower change that follows first-order kinetics consistent with intramolecular oxidation of Os^{II} by Ru^{III} for which $\Delta G° = -0.42$ eV. The kinetics are first order with $k(295 \pm 2$ K, $\mu = 0.035$ M$) = 5.3 \pm 0.9 \times 10^6$ s^{-1} in solutions 10^{-3} mM in polymer. This rate constant is slower by ~6 than the estimated rate constant for self-exchange within an association complex of $[Ru(bpy)_3]^{2+}$ and $[Ru(bpy)_3]^{3+}$ under the same conditions. At higher concentrations ($>1 \times 10^{-3}$ mM) there is evidence for intermolecular oxidation of Os^{II} by Ru^{III}.

Introduction

The coupling of single photon, single electron transfer events to multi-electron targets such as the oxidation of water or the reduction of carbon dioxide is largely an unsolved problem in artificial photosynthesis.[1] Single electron transfer photochemistry has been demonstrated for the metal-to-ligand charge transfer (MLCT) excited states of polypyridyl complexes such as $[Ru(bpy)_3]^{2+}$ (bpy = 2,2′-bipyridine),[2] the π–π^* excited states of porphyrins,[3] and organic donor–acceptor pairs.[4]

The photochemical generation of products which are oxidized or reduced by more than one electron in well-defined systems has been more elusive.[1,5a] One promising approach to this problem is by the deliberate synthesis of molecular assemblies containing multiple sites in order to achieve light absorption, electron/energy transfer, and multi-electron redox chemistry.[5,6] Soluble polymers can serve this role, and a number of photochemical electron transfer assemblies based on polymers have been reported.[7-10]

In previous work, we described the derivatization of styrene/chloromethylstyrene copolymers with pendant polypyridyl complexes and electron or energy transfer quenchers.[11] The attachment chemistry was based on nucleophilic displacement of chloride by complexes containing 4-methyl-4′-(hydroxymethyl)-2,2′-bipyridine (bpy-CH_2OH), or a carboxylato derivative, under basic conditions. In initial studies the polymers were prepared with *meta,para* mixtures of (chloromethyl)styrene. A number of photoprocesses have been studied based on the *meta,para* polymers in solution. They include examples of intra- or intermolecular

(1) (a) *Photoinduced Electron Transfer*, Part C; Fox, M. A., Chanon, M., Eds.; Elsevier: New York, 1988. (b) Meyer, T. J. *Acc. Chem. Res.* **1989**, *22(5)*, 163. (c) *Energy Resources Through Photochemistry and Catalysis*; Grätzel, M., Ed.; Academic Press: New York, 1983. (d) McLendon, G., et al. In *Photochemical Energy Conversion*; Proc. Int. Conf. Photochem. Convers. Solar Energy Storage; Elsevier: New York, 1989. (e) Kaneko, M. *Kogyo Zairyo* **1991**, *39(13)*, 33. (f) Tanaka, K. *Kagaku (Kyoto)* **1991**, *46(5)*, 313.

(2) (a) Watts, R. J. *Commun. Inorg. Chem.* **1991**, *11(5–6)*, 303. (b) Meyer, T. J. *Pure Appl. Chem.* **1990**, *62*, 1003. (c) Schmehl, R. H.; Ryu, K. C.; Ferrere, S.; Elliott, C. M. *Adv. Chem. Ser.* **1990**, *226*, 211. (d) MacQueen, D. B.; Schanze, K. S. *J. Am. Chem. Soc.* **1991**, *113*, 7470.

(3) (a) Gust, D.; Moore, T. A.; Moore, A. L.; et al. *J. Am. Chem. Soc.* **1991**, *113*, 3638. (b) Wasielewski, M. R.; Gaines, G. L., III; O'Neil, M. P.; Svec, W. A.; Niemczyk, M. P. *J. Am. Chem. Soc.* **1990**, *112*, 4559. (c) Nakamura, H.; Uehata, A.; Motonaga, A.; Ogata, T.; Nakao, S.; Nagamura, T.; Matsuo, T. *Chem. Lett.* **1988**, 1615. (d) Sessler, J. L.; Johnson, M. R.; Lin, T.-Y.; Creager, S. E. *J. Am. Chem. Soc.* **1988**, *110*, 3659. (e) Brun, A. M.; Harriman, A.; Heitz, V.; Sauvage, J.-P. *J. Am. Chem. Soc.* **1991**, *113*, 8657.

(4) (a) Bolton, J. R.; Mataga, N.; McLendon, G. *Adv. Chem. Ser.* **1991**, *228*, 1. (b) Kavarnos, G. J.; Turro, N. J. *Chem. Rev.* **1986**, *86*, 401. (c) Closs, G. L.; Calcaterra, L. T.; Green, N. J.; Penfield, K. W.; Miller, J. R. *J. Phys. Chem.* **1986**, *90*, 3673. (d) Brun, A. M.; Hubig, S. M.; Rodgers, M. A. J.; Wade, W. H. *J. Phys. Chem.* **1990**, *94*, 3869.

(5) (a) Scandola, F.; Balzani, V., Eds. *Supramolecular Photochemistry*; Ellis Horwood Ltd.: Chesson, 1991. (b) Mecklenberg, S.; Peek, B. P.; Erickson, B.; Meyer, T. J. *J. Am. Chem. Soc.* **1991**, *113*, 8540. (c) Bignozzi, C. A.; Argazzi, R.; Chiorboli, C.; Scandola, F. *Coord. Chem. Rev.* **1991**, *111*, 261. (d) Petersen, J. D.; Morgan, L. W.; Hsu, L.; Billadeau, M. A.; Ronco, S. E. *Coord. Chem. Rev.* **1991**, *111*, 319. (e) Denti, G.; Serroni, S.; Campagna, S.; Ricevuto, V.; Balzani, V. *Coord. Chem. Rev.* **1991**, *111*, 227. (f) Wasielewski, M. R. *Chem. Rev.* **1992**, *30(1)*, 435.

(6) (a) Gust, D.; Moore, T. A. *Science* **1990**, *248*, 199. (b) Gust, D.; Moore, T. A. *Science* **1989**, *244*, 35. (c) Lindsey, J. S.; Brown, P. A.; Siesel, D. A. *Tetrahedron* **1989**, *45(15)*, 4845.

(7) (a) Guillet, J. *Polymer Photophysics and Photochemistry*; Cambridge University Press: Cambridge, 1985. (b) Phillips, D. *Polymer Photophysics*; Chapman and Hall Ltd.: New York, 1985.

(8) (a) Forster, R. J.; Vos, J. G. *Macromolecules* **1990**, *23*, 4372. (b) Whitten, D. G.; Spooner, S. P.; Hsu, Y. *React. Polym.* **1991**, *15*, 37. (c) Toshihiro, Y.; Moriyasu, S. *Inorg. Chim. Acta* **1990**, *172(2)*, 131. (d) Ennis, P. M.; Kelley, J. M. *J. Phys. Chem.* **1989**, *93*, 5735. (e) Toshihiro, Y. *Polyhedron* **1986**, *5(1–2)*, 79.

(9) (a) Webber, S. E. *Chem. Rev.* **1990**, *90*, 1469. (b) Webber, S. E.; Batteas, J. D.; Kamioka, K.; Chatterjee, P. K. *J. Phys. Chem.* **1991**, *95*, 960. (c) Guillet, J. E. *Pure Appl. Chem.* **1991**, *63(7)*, 917.

(10) Baxter, S. M.; Jones, W. E., Jr.; Danielson, E.; Worl, L. A.; Younathan, J.; Strouse, G. F.; Meyer, T. J. *Coord. Chem. Rev.* **1991**, *111*, 47.

(11) (a) Younathan, J. N.; McClanahan, S. F.; Meyer, T. J. *Macromolecules* **1989**, *22*, 1048. (b) Margerum, L. D.; Meyer, T. J.; Murray, R. W. *J. Phys. Chem.* **1986**, *90(12)*, 2696.

0002-7863/93/1515-7363$04.00/0

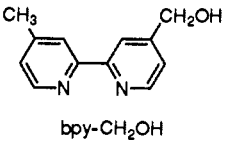

bpy-CH_2OH

electron and energy transfer,[12] the buildup of multiple redox equivalents on single polymeric strands,[13,14] and long-range energy transfer.[15]

More recently, the pure *para* isomer has been used; the structure of the repeating unit in the polymeric strands is shown below.[10,15]

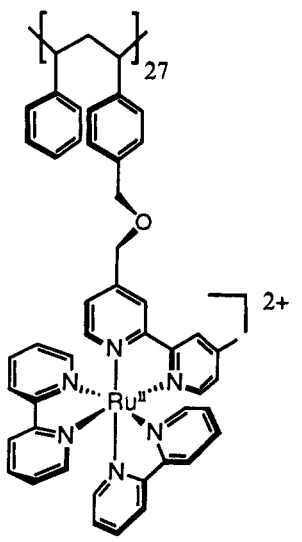

With the pure *para* isomer and a polymeric sample in which, on the average, there are ~27 chloromethyl sites, it has been possible to prepare polymers in which there are up to ~27 attached Ru^{II} or Os^{II} complexes, i.e. $[p\text{-PS-}Ru^{II}_{27}](PF_6)_{54}$ or $[p\text{-PS-}Os^{II}_{27}](PF_6)_{54}$. These abbreviations define the number of derivatized (chloromethyl)styrene groups of the ~27 available on an average polymeric strand, having the *para* geometry at the styryl substituent. With this synthetic chemistry it is possible to prepare polymers containing different groups randomly distributed along individual polymeric strands (e.g., $[p\text{-PS-}Ru^{II}_{22}Os^{II}_{5}](PF_6)_{54}$) via sequential derivatization/purification cycles.

As a prelude to the synthesis of even more complex, multifunctional assemblies, it became important to establish intrastrand properties of these polymers with regard to electron and energy transfer. For example, if a polymeric array were to be useful as a light-harvesting apparatus, mechanisms would be needed for channeling redox or excited state equivalents to a remote (catalytic) site on the polymeric backbone. In order to meet this requirement, a series of rapid electron or energy transfer steps must occur between sites on individual polymeric strands.

Described here are a series of experiments designed to investigate intrastrand electron and energy transfer in $[p\text{-PS-}Ru^{II}_{22}Os^{II}_{5}](PF_6)_{54}$. In this Ru^{II}-rich polymer, light absorptivity is dominated by MLCT absorption bands at Ru^{II}. The lowest Os^{II}-based MLCT state is lower in energy than Ru^{II*} by ~0.36 eV and Ru^{III} is a stronger oxidant than Os^{III} by 0.42 eV. Following laser flash excitation at Ru^{II}, energy transfer from Ru^{II*} to Os^{II} can be monitored by time-resolved emission and electron transfer by absorption following oxidative quenching of Ru^{II*}.

Experimental Section

Materials. Spectral grade acetonitrile (Burdick and Jackson) was used as received and stored under an Ar atmosphere. Dimethyl sulfoxide (DMSO) was distilled from KOH under reduced pressure and stored under Ar. The quencher $[4\text{-}MeOC_6H_4N_2]BF_4$ ($[ArN_2](BF_4)$), obtained from Aldrich, was stored in the dark, in a freezer, and used as received. *p*-(Chloromethyl)styrene was purchased from Kodak and distilled from KOH to remove inhibitors.

Preparation of the Styrene/*p*-(Chloromethyl)styrene Copolymer. The copolymer was prepared by a modified method of Arshady et al.,[16] which involved AIBN-initiated free radical polymerization of 1:1 styrene and *p*-(chloromethyl)styrene in chlorobenzene. The polymer is atactic and from gel permeation chromatography (GPC) the polydispersity (M_w/M_n) of the sample was 1.54 with M_n = 7011 and M_w = 10846. From the number average molecular weight the average degree of polymerization was n = 27.

Preparation of $[p\text{-}Os^{II}_{5}](PF_6)_{10}$. The polymer $[p\text{-PS-}Os^{II}_{5}](PF_6)_{10}$ was prepared similarly to the procedure described previously.[13] To a solution containing $[p\text{-PS}]_{27}$ (500 mg, 3.70×10^{-5} mmol) and $[Os(bpy)_2(bpy\text{-}CH_2OH)](PF_6)_2$ (184 mg, 1.85×10^{-4} M) in 3 mL of DMSO was added $CsOH\cdot H_2O$ (55 mg, 3.70×10^{-4} mmol). The dark red solution was stirred under Ar for 24 h and then chromatographed twice on Sephadex LH-20 (eluted with acetonitrile). The solution was concentrated and dropped into a rapidly stirred aqueous NH_4PF_6 solution to precipitate a red-black solid which was collected and washed with H_2O, Et_2O, and finally a small quantity of MeOH. The red-black solid was dried in vacuo overnight.

Preparation of $[p\text{-}Ru^{II}_{22}Os^{II}_{5}](PF_6)_{54}$. The Ru^{II}/Os^{II} polymer was prepared by reaction of the intermediate $[p\text{-PS-}Os^{II}_{5}](PF_6)_{10}$ polymer with a 3.3 molar excess of $[Ru(bpy)_2(bpy\text{-}CH_2OH)](PF_6)_2$. To a solution containing $[p\text{-PS-}Os^{II}_{5}](PF_6)_{10}$ (100 mg, 9.4×10^{-3} mmol) and $[Ru(bpy)_2(bpy\text{-}CH_2OH)](PF_6)_2$ (279 mg, 0.31 mmol) in 3 mL of DMSO was added $CsOH\cdot H_2O$ (100 mg, 0.6 mmol). The dark red solution was stirred under Ar for 24 h and then chromatographed twice on Sephadex LH-20 (eluted with acetonitrile). The solution was concentrated and dropped into a rapidly stirred aqueous NH_4PF_6 solution to precipitate a red-black solid which was collected on a frit and washed with H_2O, Et_2O, and finally a small quantity of MeOH. The red-black solid was dried in vacuo overnight.

Preparation of $[p\text{-PS-}Ru^{II}_{27}](PF_6)_{54}$ and $[p\text{-PS-}Os^{II}_{27}](PF_6)_{54}$. The polymers $[p\text{-PS-}Ru^{II}_{27}](PF_6)_{54}$ and $[p\text{-PS-}Os^{II}_{27}](PF_6)_{54}$ were prepared by procedures analogous to those described above but by allowing the *para* polymer to react with an excess (1.5×) of $[M(bpy)_2(bpy\text{-}CH_2OH)](PF_6)_2$ (M = Ru, Os).

Measurements. ^1H NMR spectra were obtained on a Brüker AC-200 spectrometer with the deuterated solvent as the reference. Gel permeation chromatography (GPC) was performed on a 860/V2.3 Waters Chromatography GPC with polystyrene weight standards. Elemental analyses for C, H, N, and Cl were performed by Oneida Laboratories. Satisfactory elemental analyses were obtained for all of the polymeric samples to ±1% in C, H, N, and Cl.

Electrochemical data were obtained by cyclic voltammetry with a PAR Model 173 potentiostat and a triangular waveform generator with the output plotted on a Hewlett-Packard 7015 XY recorder. The measurements were in acetonitrile solutions containing 0.1 M tetra-*n*-butylammonium hexafluorophosphate, $[N(n\text{-}Bu)_4](PF_6)$, as the supporting electrolyte at 295 ± 2 K, with a Pt-working and a Pt-wire auxiliary electrode. Solutions were deaerated with, and kept under a positive pressure of, Ar during each run. Potentials are referenced to the saturated sodium calomel electrode (SSCE).

UV–visible spectra were recorded on a Cary 14 interfaced to a PC by On-Line-Instruments-System, Inc. or on a Hewlett-Packard 9451A UV/Vis-diode array spectrophotometer at 295 ± 2 K.

Steady state emission measurements with 420-nm excitation were made on a SPEX Fluorolog-212A spectrofluorimeter equipped with a 450W Xenon lamp and a 10-stage, cooled Hamamatsu R636 photomultiplier tube. Relative emission quantum yields were determined at 295 ± 2 K

(12) (a) Younathan, J. N.; Jones, W. E., Jr.; Meyer, T. J. *J. Phys. Chem.* **1991**, *95*, 488. (b) Olmstead, J., III; McClanahan, S. F.; Danielson, E.; Younathan, J. N.; Meyer, T. J. *J. Am. Chem. Soc.* **1987**, *109*(*11*), 3297.

(13) (a) Worl, L. A.; Strouse, G. F.; Younathan, J. N.; Baxter, S. M.; Meyer, T. J. *J. Am. Chem. Soc.* **1990**, *112*, 7571. (b) L. Worl, Ph.D. Dissertation, University of North Carolina, Chapel Hill, 1989.

(14) Jones, W. E., Jr. Ph.D. Dissertation, University of North Carolina, Chapel Hill, 1991.

(15) (a) Strouse, G. F.; Worl, L. A.; Younathan, J. N. *J. Am. Chem. Soc.* **1989**, *111*, 9101. (b) Baxter, S.; Jones, W.; Strouse, G.; Meyer, T. manuscript in preparation.

(16) Arshady, R.; Reddy, B. S. R.; George, M. H. *Polymer* **1984**, *24*, 2749.

(17) (a) Parker, C. A.; Rees, W. T. *Analyst* (*London*) **1960**, *85*, 587. (b) Allen, G. H.; White, R. P.; Rillema, D. P.; Meyer, T. J. *J. Am. Chem. Soc.* **1984**, *106*, 2613. (c) Caspar, J. V.; Meyer, T. J. *J. Am. Chem. Soc.* **1983**, *105*, 5583.

in dilute (OD ~ 0.1) acetonitrile solutions by relative actinometry by using eq 1.[17a] In this equation Φ is the emission quantum yield of either the known or unknown (subscript 1 or 2 respectively), I is the integrated

$$\Phi_2 = \Phi_1\left(\frac{I_2}{I_1}\right)\left(\frac{n_2}{n_1}\right)^2\left(\frac{A_1}{A_2}\right) \quad (1)$$

sum of the emission intensity, n is the refractive index of the solvent, and A is the absorbance in a 1 cm cuvette cell. The reference quantum yield was $\Phi_{em} = 0.062$ for $[Ru(bpy)_3]^{2+}$ in acetonitrile.[17b,c] Time-resolved emission measurements were made by using a PRA LN1000/LN102 nitrogen laser/dye laser combination for excitation ($\lambda = 457$ nm, Coumarin 460). Emission was monitored at right angles by using a PRA B204-3 monochromator and a cooled, 10-stage Hamamatsu R928 photomultiplier. The output from the PMT was terminated through 50 Ω to a LeCroy 6880 digitizer with a LeCroy 350 MHz amplifier or a LeCroy 9400 125 MHz digitizing oscilloscope. Either digitizer was interfaced to a personal computer, with software of our own design, for data analysis and workup.

Optical densities of ~0.1 were used in all cases and the samples were deaerated by Ar purge for a minimum of 10 min or were subjected to >4 freeze–pump–thaw degassing cycles at 5×10^{-6} Torr. Time-resolved emission spectra were obtained on a point-by-point basis at 10-nm intervals with 1-mm slits. The intensity was *not* corrected for instrument response. In the emission quenching experiments the samples were bubble deoxygneated with Ar for a minimum of 10 min.

Transient absorption measurements were conducted with a system partially described elsewhere.[18a] The system incorporates a Quanta Ray DCR-2A Nd:YAG laser with the third harmonic of the fundamental separated and coupled to a Quanta Ray PDL-2 dye laser. The excitation beam was either perpendicular to or co-axial (by using appropriate dichroic optics from CVI East) with an Applied Photophysics laser kinetic spectrometer with a 250W pulsed Xenon lamp, f3.4 monochromator, and a Hamamatsu R446 photomultiplier tube. The output of the photomultiplier was coupled to either LeCroy 9400 or 6880 digitizing oscilloscopes which had been interfaced to a personal computer. Electronic synchronization and control of the experiment was achieved through electronics of our own design.[18a]

Samples for transient absorption measurements were prepared with varying concentrations of polymer ($0.4–6.0 \times 10^{-6}$ M in polymer) and $[4\text{-}MeOC_6H_4N_2](PF_6)$ as quencher ($0.0–71.0 \times 10^{-3}$ M) in acetonitrile solution at 295 ± 2 K. In each case oxygen was removed from the system by purging for at least 10 min with solvent-saturated Ar or by subjecting the solutions to a minimum of 4 freeze–pump–thaw cycles; either method proved to be sufficient for reproducing the transient absorption data. All sample preparations were conducted in the absence of light.

Steady-state photolysis measurements were conducted on a Photonics Technologies International L-1 Illumination system with a single monochromator and a 75W xenon lamp. UV/vis spectra were recorded on a Hewlett-Packard 8451A diode array spectrometer at 30-s intervals. Samples for photolysis were 35 mM in $[4\text{-}MeOC_6H_4N_2](PF_6)$ (Aldrich) and $5–6 \times 10^{-3}$ mM in polymer (~0.13 mM in Ru^{II}, ~0.03 mM in Os^{II}).

Kinetic analysis of the transient absorption and emission data was conducted by using software developed locally[18a] based on a modified Levenberg-Marquardt non-linear least-squares, iterative fitting procedure.[19] The best fit to the data was judged by following the sum of the squared errors and visually monitoring the residuals. The data were analyzed as absorbance change (ΔA) vs time traces where the absorbance change was related to the initial intensity (I_o) and the change in intensity (ΔI) by $\Delta A = \log[I_o/(I_o + \Delta I)]$.

(18) (a) Danielson, E. In preparation. (b) The full details of these calculations will appear elsewhere (Danielson, E. In preparation). In brief, the hydrocarbon backbone of the polystyrene was optimized with the Tripos Version 5.1 force field (Clark, M.; Cramer, R. D., III; Opdenbosch, N. V. *J. Compt. Chem.* **1989**, *10*, 982). Dicationic "dummy atoms" of radius 7 Å were introduced and the structure was again minimized. After minimization the molecular coordinates were exported to a user written, electrostatic optimization routine employing the modified simplex method (Nelder, J.; Mead, R. *Comp. J.* **1965**, *1*, 308.). After each step of the simplex routine the molecule was returned to the Tripos program to ascertain the energetic cost to the hydrocarbon chain that resulted from electrostatic minimization. The iterative loop was continued until a "minimum" was found. The steric energy of the backbone was dominated by the electrostatic minimization.

(19) (a) Seber, G. A.; Wild, C. J. *Non-Linear Regression*; Wiley: New York, 1987. (b) Levenberg, K. *Q. Appl. Math.* **1944**, *2*, 164. (c) Marquardt, D. W. *J. Soc. Ind. Appl. Math* **1963**, *11*, 431.

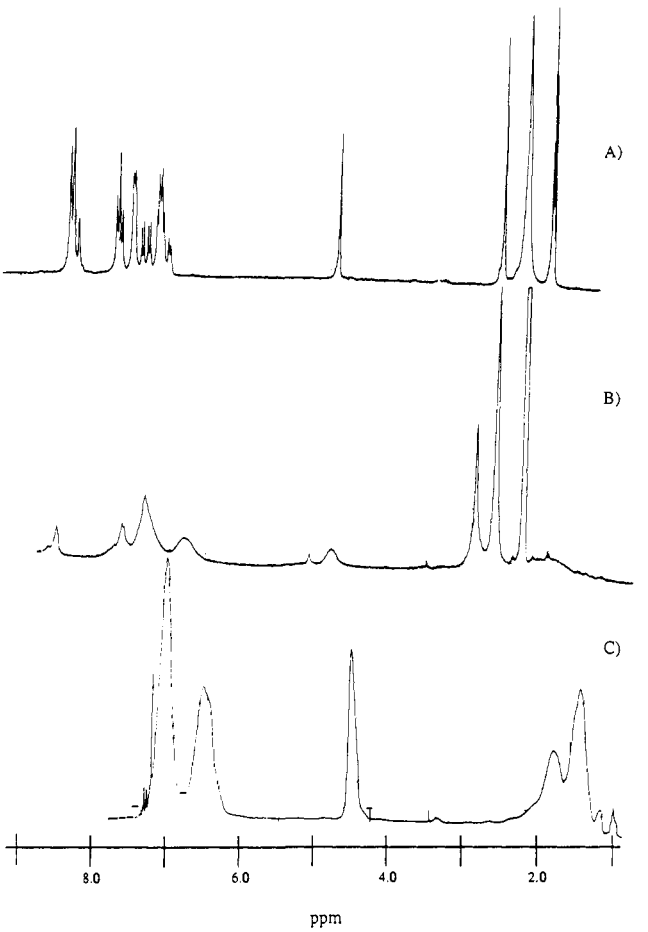

Figure 1. ^1H NMR spectra in CD_3CN (relative to CHD_2CN) for $[Ru(bpy)_2(bpy\text{-}CH_2OH)](PF_6)_2$ (A), $[p\text{-}Ru^{II}_{27}](PF_6)_{54}$ (B), and 1:1 styrene/*p*-(chloromethyl)styrene (in $CDCl_3$) (C).

Results

The Polymer. The ^1H NMR spectra for the *para* polymer are reminiscent of those for the *meta,para* polymers prepared earlier and the same procedures were used to determine the extent of polymer loading.[11] In Figure 1 are shown ^1H NMR spectra in CD_3CN for the unsubstituted 1:1 *p*-polystyrene:(chloromethyl)-styrene polymer, for $[Ru(bpy)_2(bpy\text{-}CH_2OH)](PF_6)_2$, and for $[p\text{-}PS\text{-}Ru^{II}_{27}](PF_6)_{54}$. The resonances of the polymer are broad, but it is still possible to estimate the degree of loading of the complexes by the integrated ratios of the aromatic region between 8.6 and 6.2 ppm (integration of ~23) with those for the methylene linkage at 4.5 ppm (integration of ~4) and the methyl group on bpy-CH_2OH at 2.6 ppm (integration of ~3). The benzylic resonances are shifted by 0.2 ppm on binding, allowing for detection of unreacted monomer (4.7 ppm). The latter accounts for less than 0.5% of the total complex by integration.

Half-wave potentials for the metal-based $M^{III/II}$ couples in $[p\text{-}PS\text{-}Ru^{II}_{27}](PF_6)_{54}$, $[p\text{-}PS\text{-}Os^{II}_{27}](PF_6)_{54}$, and $[p\text{-}PS\text{-}Ru^{II}_{22}Os^{II}_5](PF_6)_{54}$ were measured by cyclic voltammetry in 0.1 M $[N(n\text{-}Bu)_4](PF_6)/CH_3CN$ solutions vs SSCE. The results are reported in Table I, along with values for the constituent complexes. The peak current ratios for the $Ru^{III/II}$ and $Os^{III/II}$ couples in the mixed sample were consistent with the 4–5:1 Ru^{II}:Os^{II} ratio.

Absorption spectra for $[p\text{-}PS\text{-}Ru^{II}_{27}](PF_6)_{54}$ and $[PS\text{-}Os^{II}_{27}](PF_6)_{54}$ at room temperature in CH_3CN are shown in Figure 2, spectra A and B, respectively. In the UV (<350 nm) the spectra are dominated by $\pi \rightarrow \pi^*$ bands localized on bpy and polystyrene. In the visible, $d\pi(M^{II}) \rightarrow \pi^*$(bpy) MLCT bands appear with maxima at 456 nm for Ru and 486 nm for Os, Table I. Additional absorption maxima appear as shoulders at 433 nm for Ru and 376, 446, and 600 nm for Os. These bands are similar in profile

Table I. Properties of the Derivatized Polymers at 295 ± 2 K in CH_3CN

polymer	$E_{1/2}(M^{III/II})$,[a] V (±0.01 V)	$\lambda_{max,abs}$, nM (ϵ, M^{-1} cm^{-1} × 10^{-4}) (±1 nm)	$\lambda_{max,em}$, nm (±2 nm)	Φ_{em},[b] % (±5%)	τ_{em}, ns (±3%)
$[p\text{-PS-Ru}_{27}](PF_6)_{54}$	1.22	456 (36.1; 1.34/Ru^{II})[c]	637	0.019	809[d]
$[p\text{-PS-Os}_{27}](PF_6)_{54}$	0.81	486 (32.7; 1.21/Os^{II})[c]	755	0.0009	43
$[p\text{-PS-Ru}_{22}Os_5](PF_6)_{54}$	1.23, 0.81	456 (33.4)	633	0.018	899[d]
$[Ru(bpy)_2(bpy\text{-}CH_2OH)](PF_6)_2$	1.15	456 (1.34)	639	0.046	1036
$[Os(bpy)_2(bpy\text{-}CH_2OH)](PF_6)_2$	0.80	485 (1.30)	760	0.0030	45

[a] From cyclic voltammetric measurements at a 0.03 cm^2 Pt electrode vs SSCE in 0.1 M $[N(n\text{-}Bu)_4](PF_6)/CH_3CN$. [b] Determined by relative actinometry by using $[Ru(bpy)_3](PF_6)_2$ as the standard.[17c] [c] The molar extinction coefficients are reported both per polymer (first entry) and per chromophoric unit. [d] These values are average decay times determined by numerical integration of the first moment of the emission decay curve fit to eq 3, see text. For $[p\text{-Ru}_{22}Os_5](PF_6)_{54}$ there was also a short-lived, low-intensity, low-energy component, see text.

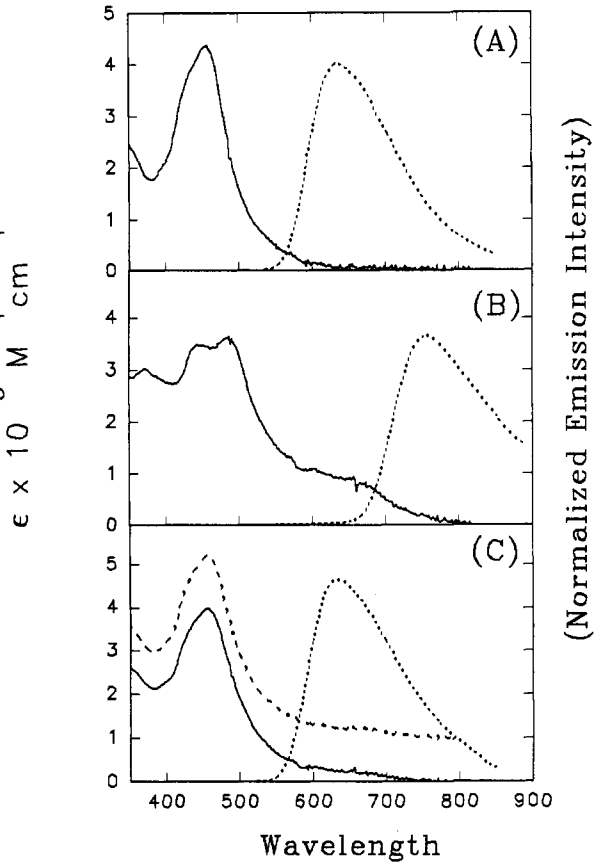

Figure 2. Absorption and emission spectra (dotted lines; 460-nm excitation; arbitrary intensity axis) for $[p\text{-}Ru^{II}_{27}](PF_6)_{54}$ (A), $[p\text{-}Os^{II}_{27}](PF_6)_{54}$ (B), and $[p\text{-PS-}Ru^{II}_{22}Os^{II}_5](PF_6)_{54}$ (C) in acetonitrile at 295 ± 2 K. The dashed line in (C) is the absorption spectrum calculated from the spectra in (A) and (B) by using eq 2. It has been offset by 10^5 molar extinction units for clarity. The molar extinction coefficients are per polymer.

and absorptivity to those for $[Ru(bpy)_2(bpy\text{-}CH_2OH)]^{2+}$ or $[Os(bpy)_2(bpy\text{-}CH_2OH)]^{2+}$.

The absorption spectrum of $[p\text{-PS-}Ru^{II}_{22}Os^{II}_5](PF_6)_{54}$ (Figure 2C) is dominated by Ru^{II} with the low-energy $d\pi(Os^{II}) \rightarrow \pi^*(bpy)$ band apparent at high concentrations. The spectrum shown as the dashed line in Figure 2C was calculated from the 22:5 statistical loading of the polymer, the per Ru^{II} and per Os^{II} molar extinction coefficients for $[p\text{-PS-}Ru^{II}_{27}](PF_6)_{54}$ ($\epsilon_{\lambda,Ru^{II}}$) and $[p\text{-PS-}Os^{II}_{27}](PF_6)_{54}$ ($\epsilon_{\lambda,Os^{II}}$), and eq 2.

$$\epsilon_{\lambda,Ru/Os} = \left(\frac{22}{27}\right)\epsilon_{\lambda,Ru} + \left(\frac{5}{27}\right)\epsilon_{\lambda,Os} \qquad (2)$$

The agreement between the two shows that the absorptions of the two chromophores are relatively unperturbed by the interchange of Ru^{II} for Os^{II}, and vice versa, and reinforces the formulation $[p\text{-PS-}Ru^{II}_{22}Os^{II}_5](PF_6)_{54}$.

Steady state emission spectra for each of the polymers at room temperature in CH_3CN are also shown in Figure 2. Emission maxima and quantum yields are listed in Table I. Emission from both $[p\text{-PS-}Ru^{II}_{27}](PF_6)_{54}$ and $[p\text{-PS-}Os^{II}_{27}](PF_6)_{54}$ was slightly blue shifted and broader than that from the constituent complexes, and emission quantum yields were decreased by ~70%. Emission from $[p\text{-PS-}Ru^{II}_{22}Os^{II}_5](PF_6)_{54}$ was dominated by Ru^{II*} based on the similarities in the spectrum and quantum yield with those for $[p\text{-PS-}Ru^{II}_{27}](PF_6)_{54}$, Figure 2 and Table I.

Emission Decay, Quenching. The results of time-resolved emission measurements are also listed in Table I. The decay of Os^{II*} in $[p\text{-PS-}Os^{II}_{27}](PF_6)_{54}$ was nearly (>99%) exponential with τ = 43 ns compared to τ = 45 ns for $[Os(bpy)_2(bpy\text{-}CH_2OH)]^{2+*}$ under the same conditions. Decay of Ru^{II*} in $[p\text{-PS-}Ru^{II}_{27}](PF_6)_{54}$ was non-exponential and somewhat dependent on the excitation irradiance. This effect has been observed previously and analyzed successfully by the stretched exponential function in eq 3.[18a] In

$$I(t) = \gamma t^{(\alpha-1)}e^{-(\beta t)^\alpha} \qquad (3)$$

eq 3, $I(t)$ is the intensity of the incident light at time t, and γ, α, and β are empirical parameters which can be related to microscopic quantities depending on the model chosen. Equation 3 is the first derivative, with respect to time, of the Kohlrausch/Williams-Watts function[20] which has been derived and applied to relaxation in disordered media.[21] Excited state decay of Ru^{II*} in $[p\text{-PS-}Ru^{II}_{27}](PF_6)_{54}$ following 457-nm excitation (62 μJ/pulse) in CH_3CN is shown in Figure 3A along with the fit of the data to eq 3 with α = 0.899, β = 1.30 × 10^6, and γ = 0.155.

Excited state decay in $[p\text{-PS-}Ru^{II}_{22}{}^{II}Os_5](PF_6)_{54}$ was more complex and depended on the monitoring wavelength at early time. The decay could be fit successfully to eq 3 if the first 200 ns of the decay trace was ignored. At 640 nm, following 457-nm excitation (65 μJ/pulse), the parameters obtained from this fit were α = 0.930, β = 1.15 × 10^6, and γ = 0.581, Figure 3B. Average lifetimes ($\langle\tau\rangle$) were calculated by numerical integration of the first moment of eq 3 and are presented in Table I.[22] At shorter times (<200 ns) there was a rapid, ~50 ns decay component whose intensity increased in magnitude at longer wavelengths where Os^{II*} emission appears in $[p\text{-PS-}Os^{II}_{27}](PF_6)_{54}$. There was no resolvable risetime (τ < 10 ns) for this component while monitoring at 800 nm.

The time-resolved emission spectrum of $[p\text{-PS-}Ru^{II}_{22}Os^{II}_5]^{54+}$ in CH_3CN at room temperature is shown in Figure 4A. The data show that at early times there is an additional emitter at low energy. The insert in Figure 4B shows the normalized difference

(20) (a) Kohlrausch, R. *Ann.* **1847**, *5*, 430. (b) Williams, G.; Watts, D. C. *Trans. Faraday Soc.* **1971**, *66*, 80.
(21) (a) Scher, H.; Lax, M. *Phys. Rev.* **1973**, B7, 4491. (b) Blumen, A.; Klafter, J.; Silbey, R. *J. Chem. Phys.* **1980**, *72*, 5320. (c) Schlesinger, M. F. Fractal Time Defect Diffusion and the Williams-Watts Model of Dielectric Relaxation. In *Relaxations in Complex Systems*; Ngai, K. L., Wright, G. B., Eds.; NTIS: Springfield, 1984; pp 261–73. (d) Dissado, L. A.; Hill, R. M. *Proc. R. Soc. London* **1983**, *A390*, 131. (e) Palmer, R. G.; Stein, D. L.; Abrahams, E.; Anderson, P. W. *Phys. Rev. Lett.* **1984**, *53*, 958.
(22) The numerical integrations were performed by using the NIntegrate command in Mathematica (Version 1.2.2).

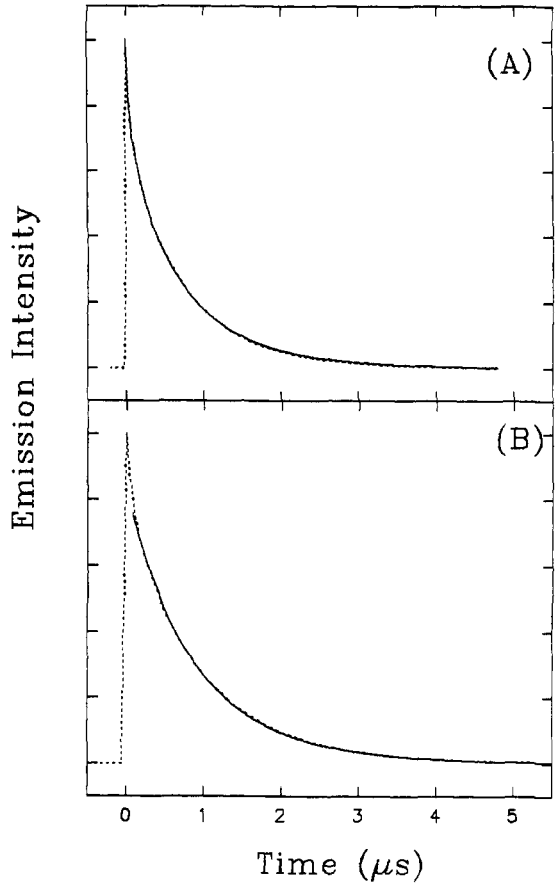

Figure 3. Emission decay traces for [*p*-Ru^{II}_{27}]$(PF_6)_{54}$ (A) and [*p*-PS-$Ru^{II}_{22}Os^{II}_5$]$(PF_6)_{54}$ (B) in CH_3CN monitored at 640 nm following 457-nm excitation (62 μJ/pulse). The overlayed (solid line) trace is a fit calculated by using eq 3 and parameters cited in the text.

between the spectra at $t \sim 0$ and 1.0 μs which provides direct evidence for a short-lived Os^{II*} emission at ~750 nm.[23]

In an earlier study it was shown that the MLCT excited states of [*m,p*-PS-Os^{II}_{30}]$(PF_6)_{60}$ and [*m,p*-PS-Ru^{II}_{30}]$(PF_6)_{60}$ underwent oxidative quenching by the diazonium salt [4-$MeOC_6H_4N_2$]BF_4 ([ArN_2]BF_4), reaction 4, with quenching rate constants of 3.2

$$[PS\text{-}M^{II}_{30}]^{60+} \xrightarrow{h\nu} [PS\text{-}M^{II}_{29}M^{II*}]^{60+} \quad (4a)$$

$$[PS\text{-}M^{II}_{29}M^{II*}]^{60+} + ArN_2^+ \rightarrow [PS\text{-}M^{II}_{29}M^{III}]^{61+} + ArN_2^{\bullet} \quad (4b)$$

$$[PS\text{-}M^{II}_{28}M^{III}M^{II*}]^{61+} + ArN_2^+ \rightarrow [PS\text{-}M^{II}_{28}M^{III}_2]^{62+} + ArN_2^{\bullet} \quad (4c)$$

(M = Ru^{II} or Os^{II})

$\times 10^9$ and 9.7×10^8 M^{-1} s^{-1}, respectively, in CH_3CN.[13] As noted in the Introduction, the *meta,para* polymer has the same repeat structure as the *para* polymer used in this study, but with a distribution of the $-CH_2-$ ring substituent between the *meta* and *para* positions. Under steady state illumination at low light intensities, sequential oxidative quenching results in the buildup of oxidative equivalents (as Ru^{III} or Os^{III}) on the individual polymeric strands, e.g. eq 4c. The fate of $ArN_2^{\bullet}$ under conditions

(23) The time-resolved emission spectra were not corrected for instrument/PMT response. This causes the apparent shift in the emission maximum relative to those reported in Table I for Os^{II*} from the steady-state measurements.

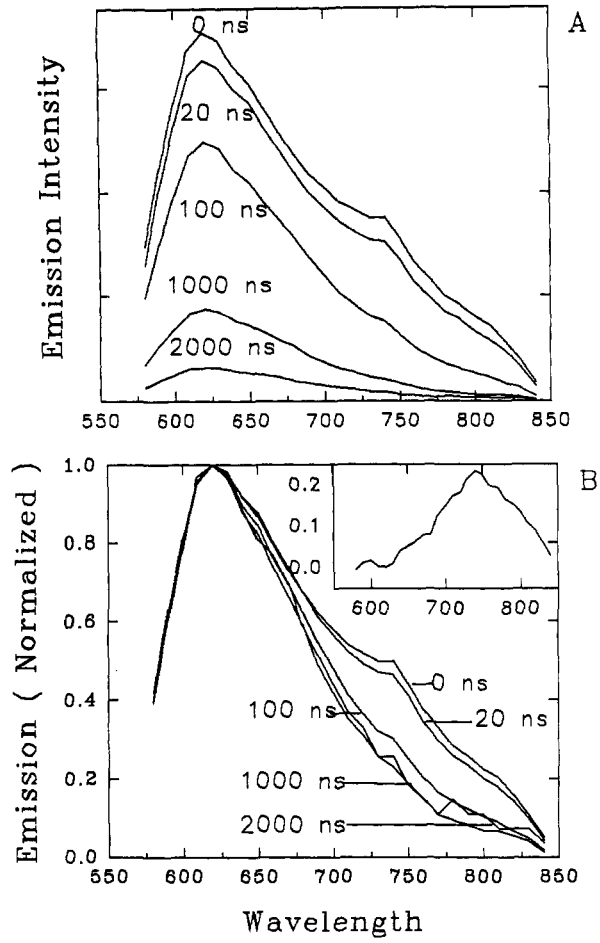

Figure 4. Time-resolved emission spectra of [*p*-PS-$Ru^{II}_{22}Os^{II}_5$]$(PF_6)_{54}$ in CH_3CN at 0, 20, 100, 1000, and 2000 ns following 457-nm excitation (155 μJ/pulse). The spectra in (A) are relative intensities and those in (B) are normalized to the emission maximum at 620 nm. The insert in (B) is the difference spectrum between the normalized spectrum at t = 0 and 1 μs.

of low illumination is loss of N_2 and H-atom abstraction by the aryl radical.[24]

The changes in absorbance that occur upon steady-state photolysis (420 nm) of CH_3CN solutions containing [*p*-PS-$Ru^{II}_{22}Os^{II}_5$]$(PF_6)_{54}$, [*p*-PS-Ru^{II}_{27}]$(PF_6)_{54}$, or [*p*-PS-Os^{II}_{27}]$(PF_6)_{54}$ (0.5×10^{-3} mM) in the presence of the diazonium salt (35 mM) were monitored by UV/visible spectroscopy, Figure 5. The traces in Figure 5 show the differences between spectra recorded after a 30-s photolysis interval and the initial spectra. For purposes of comparison the difference spectrum between [*p*-PS-Ru^{II}_{27}]$(PF_6)_{54}$ and [*p*-PS-Os^{II}_{27}]$(PF_6)_{54}$ is shown in Figure 6. From the similarities that exist in the difference spectra for [*p*-PS-$Ru^{II}_{22}Os^{II}_5$]$(PF_6)_{54}$ and [*p*-PS-Os^{II}_{27}]$(PF_6)_{54}$ after 30 s of photolysis and the difference spectrum in Figure 6, the final site of oxidation in the early stages of photolysis of [*p*-PS-$Ru^{II}_{22}Os^{II}_5$]$(PF_6)_{54}$ is at Os^{II} to give Os^{III}. This is true despite the fact that Ru^{II} is the major light absorber. The net reaction under these conditions for the first oxidative equivalent is shown in reaction 5. At longer photolysis times, the changes in the

$$[p\text{-}PS\text{-}Ru^{II}_{22}Os^{II}_5]^{54+} + ArN_2^+ \xrightarrow{h\nu} [p\text{-}PS\text{-}Ru^{II}_{22}Os^{II}_4Os^{III}]^{55+} + ArN_2^{\bullet} \quad (5)$$

difference spectra are consistent with oxidation of Ru^{II} to Ru^{III} after oxidation of Os^{II} to Os^{III} is complete, reaction 6. At the

(24) Brede, O.; Mehart, P.; Naumann, W.; Becker, H. G. O. *Ber. Bunsenges, Phys. Chem.* **1980**, *84*, 666.

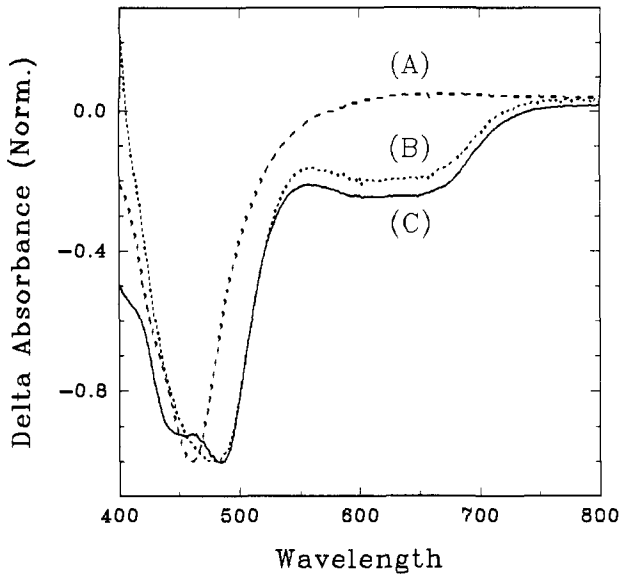

Figure 5. Difference spectra after 30 s of photolysis at 420 nm of solutions containing $[p\text{-}Ru^{II}_{27}](PF_6)_{54}$ (A), $[p\text{-}Os^{II}_{27}](PF_6)_{54}$ (B), and $[p\text{-PS-}Ru^{II}_{22}Os^{II}_{5}](PF_6)_{54}$ (C) (all at 0.5×10^{-3} mM) in CH_3CN at 295 ± 2 K in the presence of 35 mM $[4\text{-}MeOC_6H_4N_2](BF_4)$. The spectra are normalized to the same maximum negative absorbance change.

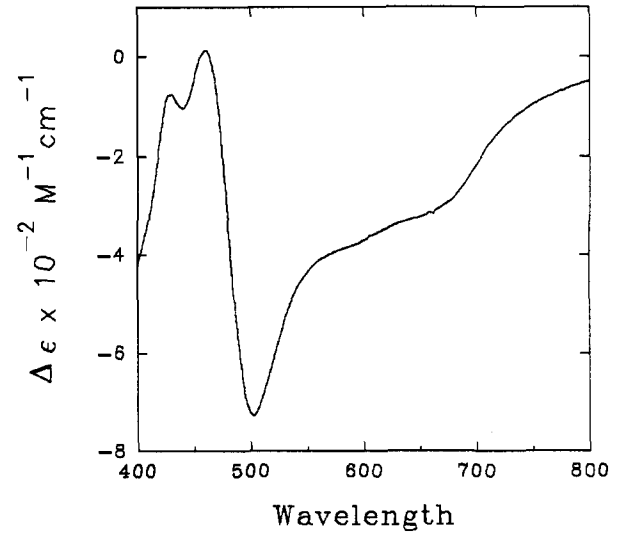

Figure 6. Absorption difference spectrum between $[p\text{-}Ru^{II}_{27}](PF_6)_{54}$ and $[p\text{-}Os^{II}_{27}](PF_6)_{54}$ in CH_3CN at 295 ± 2 K.

longest photolysis times measured (~10 min), the spectra were

$$[p\text{-PS-}Ru^{II}{}_{22}Os^{III}{}_{5}]^{59+} + ArN_2{}^{+} \xrightarrow{h\nu} [PS\text{-}Ru^{II}{}_{21}Ru^{III}Os^{III}{}_{5}]^{60+} + ArN_2{}^{\bullet} \quad (6)$$

complicated by the appearance of a new absorption feature at λ_{max} = 580 nm. It arises from a product that forms following reduction of the diazonium quencher.[24]

Transient Absorption. Transient absorption measurements were made under conditions comparable to those for steady-state photolysis (>95% emission quenching; $[ArN_2^+]$ = 35 mM) on solutions containing $[p\text{-PS-}Os^{II}_{27}](PF_6)_{54}$, $[p\text{-PS-}Ru^{II}_{27}](PF_6)_{54}$, or $[p\text{-PS-}Ru^{II}_{22}Os^{II}_{5}](PF_6)_{54}$ in CH_3CN. For $[p\text{-PS-}Os^{II}_{27}](PF_6)_{54}$ and $[p\text{-PS-}Ru^{II}_{27}](PF_6)_{54}$, the transient absorption difference spectra acquired 1 μs after 420-nm excitation (<3 mJ/pulse) were similar in form to the steady-state photolysis results in Figure 5. The absorption changes occurred within the laser pulse and there was no transient behavior. For $[p\text{-PS-}Ru^{II}_{22}Os^{II}_{5}](PF_6)_{54}$, there was an immediate absorption loss consistent with formation

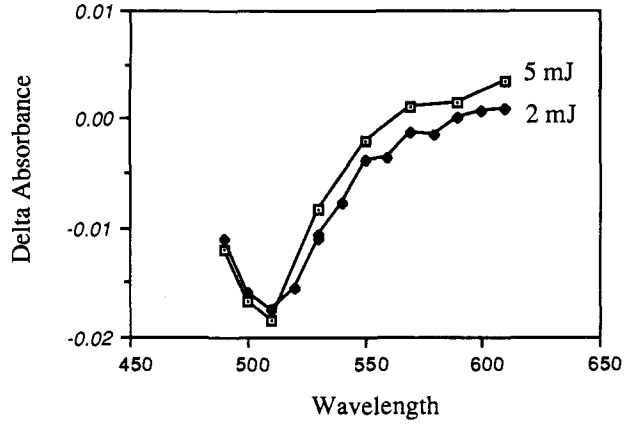

Figure 7. Absorption changes observed 1 μs after 420-nm excitation (2.0 mJ/pulse or 5.0 mJ/pulse) of a solution containing $[p\text{-PS-}Ru^{II}_{22}Os^{II}_{5}](PF_6)_{54}$ (0.05 mM) and ArN_2^+ (35 mM) in deoxygenated acetonitrile at 295 ± 2 K.

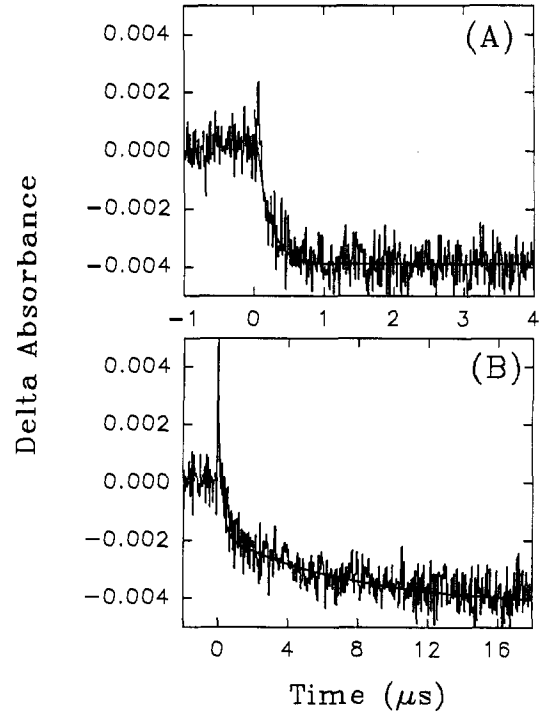

Figure 8. Transient absorption traces at 520 nm following 420-nm excitation (5 mJ/pulse) of a solution containing $[p\text{-PS-}Ru^{II}_{22}Os^{II}_{5}](PF_6)_{54}$ (0.5×10^{-6} M (A), 2.0×10^{-6} M (B)) and ArN_2^+ (35 mM) in deoxygenated acetonitrile at 295 ± 2 K. The fits to the data were to an exponential function in (A) with $k = 5.3 \times 10^6$ s^{-1} and to eq 7 for (B) with $k_1 = 4.8 \times 10^6$ s^{-1}, and $k_2 = 1.0 \times 10^5$ s^{-1}.

of Ru^{III} within the laser pulse, followed by a slower decrease in absorption at λ > 500 nm that could be time-resolved. Data acquired at 2.0 or 5.0 mJ/pulse are shown in Figure 7. The maximum change in absorption occurred at 520 nm. This wavelength corresponds to the maximum absorption difference between the pairs Ru^{III}–Os^{II} and Ru^{II}–Os^{III} as shown by the difference spectrum between $[p\text{-PS-}Os^{II}_{27}](PF_6)_{54}$ and $[p\text{-PS-}Ru^{II}_{27}](PF_6)_{54}$ in Figure 6. Ru^{III} and Os^{III} are relatively transparent in this region.

Time-resolved, transient absorption traces acquired at 520 nm following 420-nm excitation (5 mJ/pulse) of CH_3CN solutions containing $[p\text{-PS-}Ru^{II}_{22}Os^{II}_{5}](PF_6)_{54}$ and quencher are shown in Figure 8A. These absorption changes and those in Figure 7 were consistent with the prompt appearance of Ru^{III} during the laser flash followed by a time-resolvable decrease in absorption as Os^{II} was oxidized to Os^{III}. The largest transient signal in any series of experiments was obtained on the first laser flash due to the

irreversibility of the reaction and the net buildup of Os^{III} as in reaction 4. Subsequent laser flashes produced absorption changes of smaller magnitude that were similar in temporal detail. After ~20 laser flashes most of the Os^{II} sites had been oxidized to Os^{III}, and the time-resolved feature at 520 nm had disappeared.

The kinetics of the absorption changes with time were measured by using 50 mL of sample in a "tipsy cell" which allowed for sequential experiments to be conducted on fresh solutions.[25] Absorption vs time profiles obtained after the first laser flash for 10 consecutive, fresh samples were averaged to obtain the data used in the kinetic analysis. At relatively low concentrations of polymer ($\sim 0.4 \times 10^{-6}$ M), the transient behavior followed single exponential kinetics with a first-order rate constant $k_1 = 5.3 \pm 0.9 \times 10^6$ s^{-1}, Figure 8A. The precision of the determination was limited by the relatively small changes in molar extinction coefficient in the difference spectra and the difficulty in obtaining more extensively averaged data. This rate constant was measured at $\mu = 0.035$ where the electrolyte was the diazonium quencher. No attempt was made to vary the ionic strength of the solution.

At higher concentrations of polymer ($>1.0 \times 10^{-3}$ mM), the absorption decays were no longer single exponential but could be fit to the bi-exponential function in eq 7. In this expression k_1

$$I(t) = A_1 \exp[-(k_1 t)] + A_2 \exp[-(k_2 t)] \qquad (7)$$

and k_2 are characteristic decay constants and A_1 and A_2 are the fractions of the absorption change attributable to the processes described by the two exponential terms. Experiments conducted at a series of concentrations of polymer ($0.4–6.0 \times 10^{-6}$ M) revealed that the decay constant for the second term was dependent on the polymer concentration and of the following form, $k_2 = k_2'[[p\text{-PS-}Ru^{II}_{22}Os^{II}_5](PF_6)_{54}]$. Fits of the data to eq 7 gave $k_1 = 4.8 \pm 0.9 \times 10^6$ s^{-1} and $k_2' = 1.0 \pm 0.2 \times 10^5$ s^{-1}, Figure 8B.

When compared in detail, the transient absorption difference spectra for solutions containing any of the three polymers and the diazonium were dependent upon the excitation irradiance. At irradiances of <3 mJ/pulse, the initial spectra were consistent with formation of Ru^{III} only. Under these conditions the aryl radicals produced in the quenching step in reaction 4 lose N_2 and undergo further reactions (H-atom abstraction) to form organic products which do not interfere with the observed spectral changes.[24]

$$ArN_2^{\bullet} \rightarrow Ar^{\bullet} + N_2\uparrow \qquad (8)$$

At high irradiances (>3 mJ/pulse) there were shifts in the transient spectra consistent with the formation of a new species formed during the laser pulse which absorbed at $\lambda > 450$ nm. The same complication arose in an earlier pulse radiolysis study where high concentrations of $ArN_2^{\bullet}$ were generated.[24] It was attributed to a transiently stable product of the bimolecular coupling of two aryl diazyl radicals (eq 9). This intermediate appears to play a role under our conditions as well.

$$2ArN_2^{\bullet} \rightarrow Ar{-}N{=}N{-}N{=}N{-}Ar \qquad (9)$$

Discussion

Polypyridyl complexes of Ru^{II} and Os^{II} typically exhibit intense absorption bands in the visible. They arise from $d\pi(M) \rightarrow \pi^*$-(bpy) metal-to-ligand charge transfer (MLCT) transitions to give excited states which are largely singlet in character. Emission occurs from analogous states which are largely triplet in character.[26] There is a substantial amount of singlet character in the low-lying triplet states due to spin–orbit coupling at the metal.[27] The excited states are known to undergo intermolecular electron or energy transfer with a variety of quenchers.[28]

The electrochemical and photophysical properties of the complexes are largely retained in the polymers. There are special effects arising from their multi-site character,[12,13,15] but $E_{1/2}$ values and absorption and emission maxima are close to those for the model complexes $[M(bpy)_2(bpy\text{-}CH_2OH)]^{2+*}$ (M = Ru, Os). By comparing emission energies in Table I, excited state energies for $[Ru(bpy)_2(bpy\text{-}CH_2OH)]^{2+*}$ (2.17 eV) and $[Os(bpy)_2(bpy\text{-}OH)^{2+}]^*$ (1.81 eV) are also relatively unchanged on the polymers.[13,29]

Energy Transfer. In the laser flash photolysis experiments on $[p\text{-PS-}Ru^{II}_{22}Os^{II}_5](PF_6)_{54}$ in CH_3CN ~92% of the light absorbed at the excitation wavelength (460 nm) was absorbed by Ru^{II} and the remainder by Os^{II}. It was anticipated that $Ru^{II*} \rightarrow Os^{II}$ energy transfer would occur, reaction 10, since $\Delta G° = -0.36$ eV.

$$[p\text{-PS-}Ru^{II}_{22}Os^{II}_5]^{54+} \xrightarrow{h\nu} [p\text{-PS-}Ru^{II}_{21}Ru^{II*}Os^{II}_5]^{54+} \qquad (10a)$$

$$[p\text{-PS-}Ru^{II}_{21}Ru^{II*}Os^{II}_5]^{54+} \rightarrow [p\text{-PS-}Ru^{II}_{22}Os^{II}_4Os^{II*}]^{54+} \qquad (10b)$$

Creutz and Sutin have shown that intermolecular quenching of $Ru(bpy)_3^{2+*}$ by $Os(bpy)_3^{2+}$ is nearly diffusion controlled with $k = 1.5 \times 10^9$ M^{-1} s^{-1}.[30] In a more recent study by Furue et al. it was found that rapid $Ru^{II*} \rightarrow Os^{II}$ energy transfer occurred in the ligand-bridged complexes $[Ru(bpy)_2(Mebpy\text{-}(CH)_n\text{-}bpyMe)\text{-}Os(bpy)_2]^{4+}$ (n = 2, 3, 5, and 7). Energy transfer rate constants were dependent on the solvent and n, with $k = 1 \times 10^9$ s^{-1} in H_2O for $n = 2$ and 8.1×10^7 s^{-1} in CH_3CN for $n = 7$.[31,32]

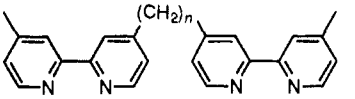

(Mebpy-$(CH_2)_n$-bpyMe)

There is evidence in the time-resolved emission spectra in Figure 4 for rapid ($\tau < 5$ ns), $Ru^{II*} \rightarrow Os^{II}$ energy transfer within the laser pulse (<5 ns) for a fraction of the Ru^{II*} excited states. The percentage emission by Os^{II*} at $t \sim 0$ was estimated by subtracting the spectrum at 1 μs (where there was no emission from Os^{II*}) from the $t \sim 0$ spectrum—the 1-μs spectrum was normalized to the maximum emission at $t \sim 0$. This procedure gave ~22% as the percent emission from Os^{II*}. On the basis of relative absorptivities, emission quantum yields, and lifetimes (Table I), emission from Os^{II*} formed by direct excitation was ~2%.[33] A considerable fraction of emission from Os^{II*} occurs from photons that were initially absorbed at Ru^{II} providing evidence for $Ru^{II*} \rightarrow Os^{II}$ energy transfer within the laser pulse ($\tau < 5$ ns, $k > 2 \times 10^8$ s^{-1}).

There was no evidence for further $Ru^{II*} \rightarrow Os^{II}$ energy transfer after the laser pulse. The low-energy feature in time-resolved emission spectra attributable to Os^{II*} no longer appeared and the average lifetime for the remaining emission from Ru^{II*} ($\langle\tau\rangle \sim$

(25) The "Tipsy Cell" was a freeze–pump–thaw degassable sample container attached to a 1-cm cuvette cell. In this device the sample solution in the cuvette can be changed while maintaining an oxygen free environment.[13]

(26) (a) Meyer, T. J. *Pure Appl. Chem.* **1986**, *58*, 1193. (b) Krausz, E.; Ferguson, J. *Prog. Inorg. Chem.* **1989**, *37*, 293. (c) Crosby, G. A.; Highland, K. A.; Trusdell, K. A. *Coord. Chem. Rev.* **1985**, *64*, 41.

(27) Kober, E. M.; Meyer, T. J. *Inorg. Chem.* **1984**, *23*, 3879.

(28) (a) Whitten, D. G. *Acc. Chem. Res.* **1980**, *13*, 83. (b) Meyer, T. J. *Prog. Inorg. Chem.* **1983**, *30*, 389. (c) Hoffman, M. Z.; Bolletta, F.; Maggi, L.; Hug, G. L. *J. Phys. Chem. Ref. Data* **1989**, *18*, 219.

(29) Lumpkin, R. Ph.D. Dissertation, The University of North Carolina, 1987. (b) Kober, E.; Worl, L.; Lumpkin, R.; Murtaza, Z.; Bates, D.; Meyer, T. J. Manuscript in preparation.

(30) Creutz, C.; Chou, M.; Netzel, T. L.; Okumura, M.; Sutin, N. *J. Am. Chem. Soc.* **1980**, *102*, 1309.

(31) Furue, M.; Yoshidzumi, T.; Kinoshita, S.; Kushida, T.; Nozakura, S.; Kamachi, M. *Bull. Chem. Soc. Jpn.* **1991**, *64*, 1632.

(32) Furue, M.; Hirata, M.; Kinoshita, S.; Kushida, T.; Kamachi, M. *Chem. Lett., Jpn.* **1990**, 2065.

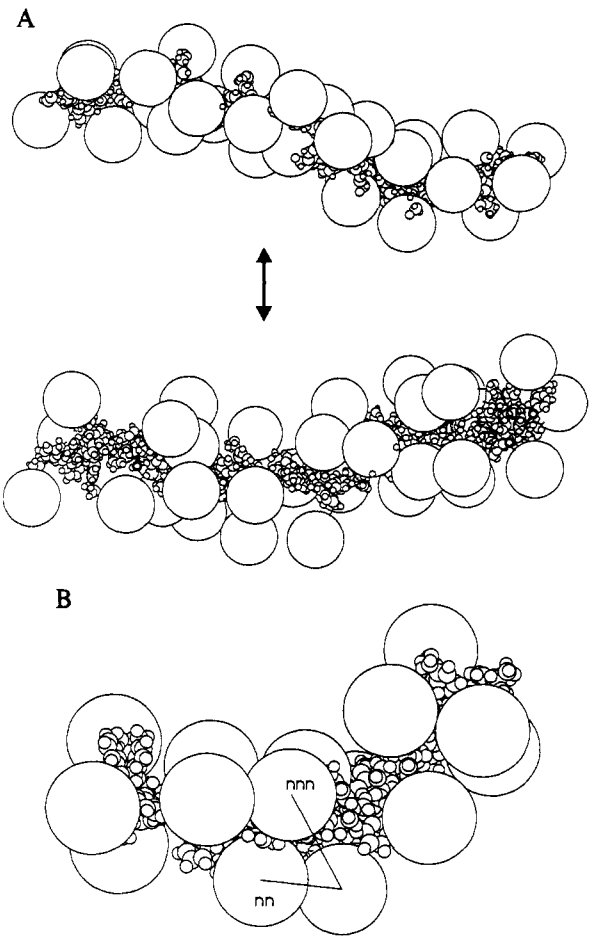

Figure 9. The results of a molecular modeling study on the polymer $[p\text{-}Ru^{II}_{30}]^{60+}$ illustrating (A) two of many low-energy conformations accessible within kT and (B) a blowup illustrating a smaller segment.[18b] The center-to-center distance between adjacent metal complex sites is 21 ± 2 Å, 7 ± 2 Å between the peripheries of the complexes. These distances are 34 ± 6 and 20 ± 6 Å respectively for non-nearest neighbors. Nearest and non-nearest neighbor distances are illustrated by the lines in Figure 9b.

899 ns) was nearly the same as for Ru^{II*} in $[p\text{-PS-}Ru^{II}_{27}](PF_6)_{54}$ ($\langle\tau\rangle \sim 809$ ns) under the same conditions.

From these observations a fraction of the Ru^{II*} excited states undergo rapid energy transfer to Os^{II} and the remainder undergo slow or no energy transfer ($\tau > 1$ μs, $k < 1 \times 10^6$ s^{-1}). Thus different Ru^{II*} excited states appear to form following excitation of $[p\text{-PS-}Ru^{II}_{22}Os^{II}_5](PF_6)_{54}$.

The results of molecular modeling calculations on $[p\text{-PS-}Ru^{II}_{30}](PF_6)_{60}$ show that the extended spatial structure of the polymer is dominated by the large (~14-Å diameter) cationic metal centers.[18b] These results are illustrated in Figure 9 in which are shown two low-energy conformations (of many within kT) of an average strand of the polymer $[p\text{-PS-}Ru^{II}_{30}]^{60+}$ and a blowup illustrating a smaller segment.

In these structures the cationic complexes enforce a spatially extended structure. In the lowest energy structures the center-to-center distance between nearest neighbors (nn in Figure 9B) is ~21 ± 2 Å, ~7 ± 2 Å between the peripheries of the complexes. There are four nearest neighbors (nnn in Figure 9B). These distances increase to 34 ± 6 and 20 ± 6 Å for non-nearest neighbors. Closer approaches, where electronic coupling would be enhanced, are accessible by local segmental motions, but their relative contribution to electron or energy transfer would be weighted by statistically decreased populations.

The mixed-metal polymer was prepared by first loading the strands with Os^{II}. If Os^{II} were uniformly distributed along the strands (in order to minimize electrostatic repulsion, for example), each pair of nearest neighbor Os^{II}'s would be separated, on the average, by 4–5 Ru^{II}'s. A segment of the resulting structure is illustrated below with the Os^{II} sites labeled with cross-hatching and assuming 5 Ru^{II} spacers between Os^{II}'s.

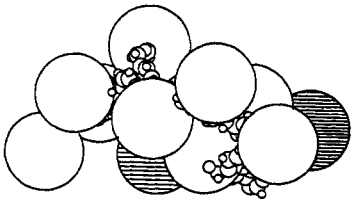

In an individual strand, with 27 sites available, ~8 of the 22 Ru^{II} sites would be adjacent to Os^{II} and ~14 non-adjacent. The actual distribution may be far more random, but in any distribution there will be ~1/3 adjacent and ~2/3 non-adjacent.

On the basis of electrochemical and spectral comparisons, there is no evidence that the exchange of Os^{II} for Ru^{II} in $[p\text{-PS-}Ru^{II}_{27}](PF_6)_{54}$ to give $[p\text{-PS-}Ru^{II}_{22}Os^{II}_5](PF_6)_{54}$ causes significant electronic perturbations. Rather, we conclude that the origin of the different behaviors for Ru^{II*} is due to the relative positioning of Ru^{II*} with respect Os^{II}, and whether initial excitation occurs at a Ru^{II} that is adjacent to or remote from Os^{II}. Various excitation possibilities are summarized in Scheme I.

Statistically ~1/3 of the excitation events produce Ru^{II*} adjacent to Os^{II}. Rapid energy transfer from these sites would explain the rapid energy transfer component. If this interpretation is correct, intrastrand $Ru^{II*} \rightarrow Os^{II}$ energy transfer is more facile than intramolecular energy transfer in Furue's ligand-bridged complexes.[31,32]

For (ii) and (iii) in Scheme I, net $Ru^{II*} \rightarrow Os^{II}$ energy transfer can occur but must be preceded by one or more $Ru^{II*} \rightarrow Ru^{II}$ energy self-exchange steps. These steps must be slow relative to the excited state lifetime of Ru^{II*} since $\langle\tau\rangle$ and ϕ_{em} for Ru^{II*} in $[p\text{-PS-}Ru^{II}_{22}Os^{II}_5](PF_6)_{54}$ are relatively unaffected compared to those in $[p\text{-PS-}Ru^{II}_{27}](PF_6)_{54}$. If $1/(k_{ex,et})$ were rapid or competitive with $\langle\tau\rangle$, significant quenching would have been observed. From these observations, we conclude that $Ru^{II*} \rightarrow Ru^{II}$ self-exchange in $[p\text{-PS-}Ru^{II}_{22}Os^{II}_5](PF_6)_{54}$ is slow with $k_{ex,et} < 1 \times 10^6$ s^{-1}.

Electron Transfer. The spectral changes that occur following conventional or laser flash photolysis of solutions containing $[p\text{-PS-}Ru^{II}_{27}](PF_6)_{54}$ or $[p\text{-PS-}Os^{II}_{27}](PF_6)_{54}$ and high (35 mM) concentrations of the diazonium quencher $[4\text{-}MeOC_6H_4N_2](BF_4)$ are consistent with initial oxidative quenching of Ru^{II*} or Os^{II*} as in reaction 4. At the quencher concentrations used, excitation and quenching occur during the laser flash. This leads to a general loss in MLCT absorption in the visible. The subsequent time-resolved changes that are observed are attributable to oxidation of Os^{II} by Ru^{III}.

A series of competing reactions may contribute to these observations, Scheme II. (1) Excitation and quenching at Os^{II} would result in Os^{III} during the laser pulse, reaction iv, in Scheme II, with no contribution to subsequent transient behavior. (2) Excitation at Ru^{II} adjacent to Os^{II}, followed by energy transfer, reaction v, and oxidative quenching, would give the same result. (3) Excitation at Ru^{II} and oxidative quenching before energy

(33) The fraction of emitted light from Os^{II*} (I_{Os}) at $t = 0$ in the absence of energy transfer was estimated from the equation,

$$\frac{I_{Os^{II*}}}{I_{Ru^{II*}} + I_{Os^{II*}}} = \frac{(A_{Os}/A_T)(\phi_{em}/\tau)_{Os}}{(A_{Os}/A_T)(\phi_{em}/\tau)_{Os} + (A_{Ru}/A_T)(\phi_{em}/\tau)_{Ru}}$$

In this equation A_{Ru}, A_{Os}, and A_T were the absorbances at the excitation wavelength (460 nm) contributed by Ru^{II} and Os^{II} and the total absorbance. The absorbances were calculated from the known molar extinction coefficients at 460 nm ($\epsilon_{Os(II)} = 1.29 \times 10^4$ M^{-1} cm^{-1}, $\epsilon_{Ru(II)} = 1.34 \times 10^4$ M^{-1} cm^{-1}). The quantum yields and lifetimes were taken from Table I. This procedure neglects the (relatively small) amount of emission decay from Os^{II*} that occurred during the laser pulse.

Scheme I

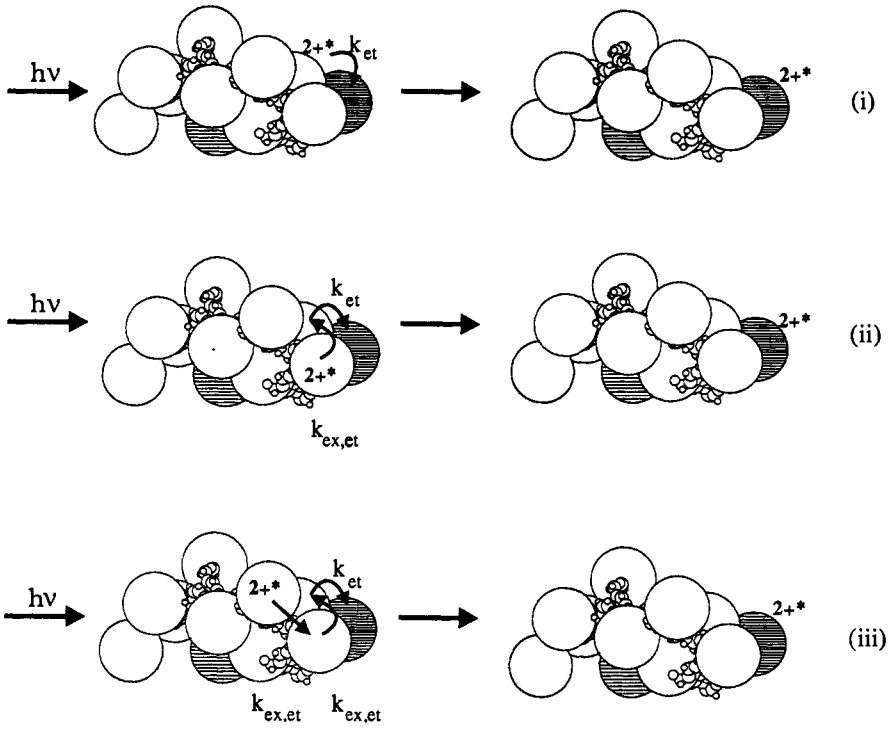

Scheme II

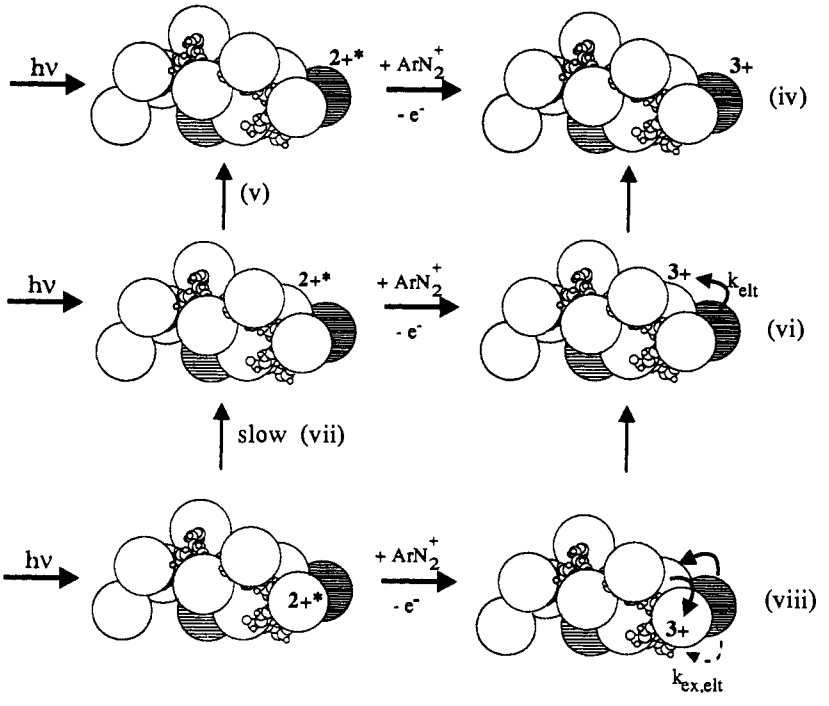

transfer would give Ru^{III} in sites adjacent to, reaction vi, or remote from Os^{II}, reaction viii. In the case of reaction vi subsequent oxidation of Os^{II} by Ru^{III} should be rapid since it is favored by 0.42 eV. In the case of reaction viii electron self-exchange from Ru^{II} to Ru^{III} would have to occur first in order to bring Ru^{III} to a site adjacent to Os^{II}.

Since energy transfer self-exchange is slow, (vii) in Scheme II, Ru^{II*}, once formed, remains where excited unless adjacent to Os^{II}. Direct excitation and quenching at Os^{II} accounts for $\sim^1/_5$ of the Os^{III} produced and it occurs within the laser pulse. Excitation at the $\sim^1/_3$ Ru^{II} sites adjacent to Os^{II} followed by energy transfer to Os^{II} and quenching also occurs during the laser pulse. It accounts for an additional $\sim^1/_3$ of the Os^{III} produced.

In solutions dilute in polymer, the remainder of the Os^{III} appears by first-order kinetics consistent with intrastrand electron transfer. Three pathways could contribute: (1) oxidation by Ru^{III} adjacent to Os^{II} (vi in Scheme III); (2) electron transfer self-exchange (viii) followed by $Os^{II} \rightarrow Ru^{III}$ electron transfer (vi); (3) long-range electron transfer from Os^{II} to non-adjacent Ru^{III} which is illustrated by the dashed arrow in viii.

There is evidence for only one transient process with k_1(298 K, μ = 35 mM) = (5.3 ± 0.9) × 10^6 s^{-1}. We presume it is dominated by rate-limiting $Ru^{II} \rightarrow Ru^{III}$ self-exchange followed

by rapid $Os^{II} \rightarrow Ru^{III}$ electron transfer. It is doubtful that long-range $Os^{II} \rightarrow Ru^{III}$ electron transfer between non-adjacent sites plays a significant role because of the large separation distance of 20 ± 6 Å (periphery to periphery) compared to 7 ± 2 Å for nearest neighbors.

The self-exchange rate constant for the $[Ru(bpy)_3]^{3+/2+}$ couple in CD_3CN (298 K, μ = 0.068 mM) is $k_{obs} = 8 \times 10^6$ M^{-1} s^{-1}.[34] From this value and an association constant of $K_A \sim 0.3$,[35a] the rate constant for electron transfer within an association complex between $[Ru(bpy)_3]^{3+}$ and $[Ru(bpy)_3]^{2+}$ is $k = k_{obs}/K_A \sim 3 \times 10^7$ s^{-1}. This is within a factor of ~6 of k_1 for intrastrand electron

$$Ru^{III}(bpy)_3^{3+},Ru^{II}(bpy)_3^{2+} \rightarrow Ru^{II}(bpy)_3^{2+},Ru^{III}(bpy)_3^{3+} \quad (11)$$

$$k = k_{obs}/K_A$$

transfer. A difference of this magnitude could be reconciled easily by recognizing that when the complexes are attached to the polymeric strands there are fewer degrees of freedom than for isolated reactants in solution. From the molecular modeling calculation, adjacent complexes are not in close contact in the energy minimized structure. The experimental rate constant for intrastrand electron transfer must represent a balance between contributions from conformations where the distance between complexes is minimized, so as to maximize electronic coupling, and statistically more probable distributions where the separation distance is larger.[36]

Adjacent $Os^{II} \rightarrow Ru^{III}$ electron transfer is probably too rapid for us to time-resolve with our apparatus. By assuming the same pre-exponential factors and reorganizational energies (λ) for $Os^{II} \rightarrow Ru^{III}$ (k_{elt}) and $Ru^{II} \rightarrow Ru^{III}$ ($k_{ex,elt}$) electron transfer, the ratio of rate constants is given by the Marcus equation in the classical limit by eq 12.[35b]

$$\frac{k_{elt}}{k_{ex,elt}} = -\left(\frac{2\lambda\Delta G^\circ + \Delta G^{\circ 2}}{4\lambda RT}\right) \quad (12)$$

With ΔG° = –0.42 eV, T = 295 K, and λ = 1.2 eV, the rate constant ratio is 1.7×10^4 and $k_{elt} = 9 \times 10^{10}$ s^{-1}.[35b]

Even if the transient event observed is dictated ratewise by $Ru^{II} \rightarrow Ru^{III}$ self-exchange, the experimental "rate constant" includes contributions from a distribution of processes. Pathways exist involving several electron jumps. An example is shown in reaction 13. (The importance of such contributors will depend on the number of electron transfer events required to reach Os^{II}, the number of sites involved, and the statistics of electron transfer toward or away from Os^{II}.)

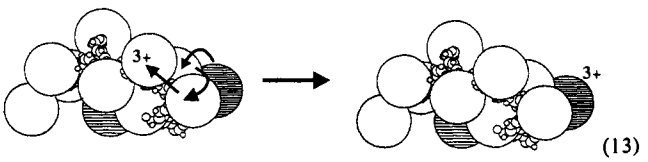

(13)

In addition, there are chemically non-equivalent sites on the polymer, and a myriad of intrastrand conformations within kT. Each could have at least slightly different rate constants for electron transfer. Multiple excitation and electron transfer quenching[13,14] would give a range of oxidative compositions during the flash, $[p\text{-PS-}Ru^{II}_{22-n}Ru^{III}_nOs^{II}_5]^{(54+n)+}$ (n = 1–5). In general, each of these could have different rate constants for intrastrand electron transfer (although k was independent of irradiance under the conditions of Figure 7).

The low quality of our data precludes resolution of the expected distribution of rate processes into separate components, and it was not possible to apply more appropriate kinetic models.[20,21] The problem was in the small absorbance changes and the concomitantly low signal-to-noise ratio.

At higher concentrations of polymer (1.0–3.0 × 10^{-6} M) interstrand electron transfer plays a role. In the biexponential fits of the kinetics data, the rate constant for intrastrand electron transfer was recovered in one term and the second term was dependent on the concentration of polymer. This behavior is consistent with competitive interstrand $Os^{II} \rightarrow Ru^{III}$ electron transfer, eq 14. Related equations can be written for bimolecular reactions involving multiply oxidized strands.

$$[p\text{-PS-}Ru^{II}_{21}Ru^{III}Os^{II}_5]^{55+} + [p\text{-PS-}Ru^{II}_{22}Os^{II}_5]^{54+} \rightarrow [p\text{-PS-}Ru^{II}_{22}Os^{II}_5]^{54+} + [p\text{-PS-}Ru^{II}_{22}Os^{II}_4Os^{III}]^{55+} \quad (14)$$

A Ru^{III} site can be reduced by any Os^{II}, regardless of whether the strand it is on contains Ru^{III}. The rate law that results from this consideration is given by eq 15 (with additional terms for other forms of the oxidized polymer, e.g. $[p\text{-PS-}Ru^{III}_2Ru^{II}_{20}Os^{II}_5]^{56+}$, to be added).

$$\begin{aligned}\text{rate} &= k_{inter}\{[[p\text{-PS-}Ru^{II}_{22}Os^{II}_5]^{54+}] + [[p\text{-PS-}Ru^{III}Ru^{II}_{21}Os^{II}_5]^{55+}] + [[p\text{-PS-}Ru^{II}_{22}Os^{II}_4Os^{III}]^{55+}] + ...\} \times [[p\text{-PS-}Ru^{III}Ru^{II}_{21}Os^{II}_5]^{55+}] \\ &= k_{inter}\{\text{total polymer concentration}\} \times [[p\text{-PS-}Ru^{III}Ru^{II}_{21}Os^{II}_5]^{55+}] \\ &= k_{obs}[p\text{-PS-}Ru^{III}Ru^{II}_{21}Os^{II}_5]^{55+} \quad (15)\end{aligned}$$

$$k_{obs} = k_{inter}\{\text{total polymer concentration}\}$$

This is true only if the contributions to k_{inter} from the various oxidation state isomers and distributions are comparable. In this limit, Os^{II} is in pseudo-first-order excess at the relatively low concentrations of $[p\text{-PS-}Ru^{III}Ru^{II}_{21}Os^{II}_5]^{55+}$ (+ $[p\text{-PS-}Ru^{III}_2Ru^{II}_{20}Os^{II}_5]^{56+}$ + $[p\text{-PS-}Ru^{III}Ru^{II}_{21}Os^{II}_4Os^{III}]^{56+}$ + ...) which are formed during the laser pulse.

On the basis of this analysis, $k_2/[\text{polymer}] = k_{inter}(CH_3CN, \mu = 35$ mM) = (3.2 ± 0.6) × 10^{10} M^{-1} s^{-1}. Rate constants of this magnitude, which are in excess of the diffusion-controlled limit of 1–2 × 10^{10} M^{-1} s^{-1} in CH_3CN, have been reported for

(34) Chan, M.-S.; Wahl, A. C. *J. Phys. Chem.* **1978**, *82*, 2542.

(35) (a) The constant $K_a \approx 0.3$ was calculated from the Eigen–Fuoss equation,[37]

$$K_A = \frac{4\pi N_o d^3}{3000}\exp^{-(w_r/RT)}$$

$$w_r = \frac{z_D z_A e^2}{D_s d}\left(\frac{1}{1+\kappa_D}\right)$$

$$\kappa_D = \left(\frac{8\pi e^2 N_o \mu}{100 D_s RT}\right)$$

in which N_0 is Avogadro's number, μ the ionic strength, D_s the static dielectric constant of the solvent, and d the sum of the donor and acceptor radii. (b) This relationship follows from the modified Marcus equation, $k = \nu \exp(-[(\lambda + \Delta G^\circ)^2/4\lambda RT])$, in which ν is the frequency factor for electron transfer, by assuming that ν and λ are the same for $Ru^{II} \rightarrow Ru^{III}$ and $Os^{II} \rightarrow Ru^{III}$ electron transfer and recalling that $\Delta G^\circ = 0$ for the $Ru^{II} \rightarrow Ru^{III}$ self-exchange. The value of λ = 1.2 eV was calculated from the $Ru(bpy)_3^{3+/2+}$ self-exchange rate constant (8.6×10^6 M^{-1} s^{-1} in CD_3CN at 298 K, μ = 0.068) from $\lambda = 4RT\ln(\nu K_A/k)$, with $\nu K_A = 10^{12}$ s^{-1}.

(36) (a) Sutin, N. *Acc. Chem. Res.* **1982**, *15*, 275. (b) Sutin, N.; Brunschwig, B. S.; Creutz, C.; Winkler, J. R. *Pure Appl. Chem.* **1988**, *60*, 1817. (c) Marcus, R. A.; Sutin, N. *Biochim. Biophys. Acta* **1985**, *84*, 265. (d) Brunschwig, B. S.; Ehrenson, S.; Sutin, N. *J. Phys. Chem.* **1986**, *90*, 3657.

other electron transfer reactions involving polymers.[7,11a,38] The very rapid rate constants arise because of the multi-site, extended molecular volume of the reactants. Once an encounter has occurred, $Os^{II} \rightarrow Ru^{III}$ electron transfer is expected to be rapid given the result of the analysis in eq 12.

Intrastrand Electron and Energy Transfer. Electron transfer self-exchange between Ru^{II} and Ru^{III} on the individual polymeric strands appears to be relatively unaffected compared to the equivalent reaction in solutions. This is not a surprising result given the electrochemical and spectral results which suggest that the polymer-bound complexes have ground and excited state properties similar to those of the component complexes in solution. By inference, solvent and intramolecular reorganizational energies at the individual redox sites in the polymer must be relatively unaffected. The decrease in rate constant that does exist may be largely a consequence of the increase in average spacing between the peripheries of adjacent redox sites from close contact in the outer-sphere reaction to 7 ± 2 Å in the polymer.[39]

Energy transfer is another matter. Our lower limit for $Ru^{II*} \rightarrow Os^{II}$ energy transfer between adjacent sites is not inconsistent with the results of Furue et al. The dominant pathway for energy transfer, whether Förster (singlet–singlet) or Dexter (triplet–triplet with spin exchange), remains unknown. The excited states are of mixed spin character with significant singlet character mixed into the largely triplet excited states by spin–orbit coupling.[27]

Quenching of Ru^{II*} by Os^{II}, which is favored by 0.36 eV, is rapid ($k > 2 \times 10^8$ s^{-1}). The puzzling result is that energy transfer self-exchange is so slow, $k < 1 \times 10^6$ s^{-1}. The rate constant for self-exchange in an association complex between $[Ru(bpy)_3]^{2+}$ and $[Ru(bpy)_3]^{2+*}$ can be calculated by using eq 16 and the results of emission spectral fitting. This equation includes contributions to the activational barrier to energy transfer by averaged, medium-frequency, ring-stretching modes in the donor (D,*n) and acceptor (A,m) and assumes equal quantum spacings ($\hbar\omega$, $\hbar\omega'$) between the participating ground and excited states (D*/D and A*/A). Low-frequency vibrations and solvent librations are treated classically, and the sum of their reorganizational energies is λ'.[40,41]

$$k_{et} = (2\pi V^2/h)F(\text{calcd}) \quad (16a)$$

$$F(\text{calcd}) = 1/(4\pi\lambda' k_B T)^{1/2} \sum_{n^*}\sum_{m} \exp[-(S_D)] \times \exp[-(S_A)(S_D^{n^*}/n^*!)(S_A^m/m!)] \times \exp[-\{(\Delta G^\circ + \lambda' + n^*h\omega' + mh\omega')^2/(4\lambda' k_B T)\}] \quad (16b)$$

In eq 16b, S_D and S_A are the electron-vibrational coupling constants between D*/D and A*/A. The sums are over the ground state vibrational levels of the acceptor (m) and the excited state vibrational levels of the donor (n^*). The quantity V is the energy exchange matrix element. Assuming equal quantum spacings in the ground and excited states ($h\omega_{n^*} = h\omega_m$) for a self-exchange process ($\Delta G^\circ = 0$, $S_D = S_A = S$), eq 16b becomes

$$F(\text{calcd}) = 1/(4\pi\lambda' k_B T)^{1/2} \sum_{n^*}\sum_{m} \exp[-(2S)(S^{n^*}/n^*!) \times (S^m/m!)] \exp[-\{(\lambda' + (n^*+m)h\omega')^2/(4\lambda' k_B T)\}] \quad (17)$$

The parameters $\lambda' = 1260$ cm^{-1}, $S = 0.99$, and $\hbar\omega = 1350$ cm^{-1} are available for $[Ru(bpy)_3]^{2+*}$ in CH_3CN based on a Franck–Condon analysis of its emission spectrum.[42] A value of $V = 2$ cm^{-1} has been estimated for the quenching of a series of Os^{II*} excited states by anthracene.[41] By using that value and the spectral fitting parameters, $k_{calcd}(298K, CH_3CN) = (3 \pm 1) \times 10^8$ s^{-1}. The experimental value is lower by at least two orders of magnitude and less than electron self-exchange by >5. From the results of Closs et al., a decrease of ~2 was found in comparing intramolecular electron and energy transfer in related systems.[43]

Slow energy transfer may be an additional consequence of the $\sim 7 \pm 2$ Å average spacing between sites and a greater sensitivity to internuclear separation for energy transfer compared to electron transfer. This effect would also exist for $Ru^{II*} \rightarrow Os^{II}$ energy transfer but be compensated, in part, by the driving force of 0.36 eV.

Acknowledgment. We gratefully acknowledge the Department of Energy for financial support under Grant DE-FG05-86ER13633 and Earl Danielson for the calculations on the structure of the polymer.

(37) (a) Eigen, M. Z. *Phys. Chem.* **1954**, *1*, 176. (b) Fuoss, R. M. *J. Am. Chem. Soc.* **1958**, *80*, 5059.
(38) (a) Webber, S. E. *Macromolecules* **1986**, *19*, 1658. (b) Chu, D. Y.; Thomas, K. *Macromolecules* **1984**, *17*, 2142.
(39) (a) Hush, N. S. *Coord. Chem. Rev.* **1985**, *64*, 135. (b) McLendon, G. *Acc. Chem. Res.* **1988**, *21*, 160. (c) Newton, M. D. *Chem. Rev.* **1991**, *91*, 767. (d) Closs, G. L.; Miller, J. R. *Science* **1988**, *240*, 440. (e) Bowler, B. E.; Raphael, A. L.; Gray, H. B. *Prog. Inorg. Chem.* **1990**, *38*, 259.
(40) (a) Ulstrup, J.; Jortner, J. *J. Chem. Phys.* **1975**, *63*, 4358. (b) Orlandi, G.; Monte, S.; Barigelletti, F.; Balzani, V. *Chem. Phys.* **1980**, *52*, 313.
(41) Murtaza, Z.; Zipp, A. P.; Worl, L. A.; Graff, D.; Jones, W. E., Jr.; Bates, W. D.; Meyer, T. J. *J. Am. Chem. Soc.* **1991**, *113*, 5113.
(42) Caspar, J. V.; Meyer, T. J. *J. Am. Chem. Soc.* **1983**, *105*, 5583.
(43) Closs, G. L.; Piotrowiak, P.; MacInnis, J. M.; Fleming, G. R. *J. Am. Chem. Soc.* **1988**, *110*, 2652.